JACS
JOURNAL OF THE AMERICAN CHEMICAL SOCIETY
Article
pubs.acs.org/JACS

Photoreaction of a Hydroxyalkyphenone with the Membrane of Polymersomes: A Versatile Method To Generate Semipermeable Nanoreactors

Mariana Spulber,[†] Adrian Najer,[†] Katharina Winkelbach,[‡] Olfa Glaied,[‡] Marcus Waser,[‡] Uwe Pieles,[‡] Wolfgang Meier,[†] and Nico Bruns*[,†]

[†]Department of Chemistry, University of Basel, Klingelbergstrasse 80, 4056 Basel, Switzerland

[‡]Institute of Chemistry and Bioanalytics, School of Life Sciences, University of Applied Sciences and Arts Northwestern Switzerland, Gründenstrasse 40, 4132 Muttenz, Switzerland

Supporting Information

ABSTRACT: Block copolymer vesicles can be turned into nanoreactors when a catalyst is encapsulated in these hollow nanostructures. However the membranes of these polymersomes are most often impermeable to small organic molecules, while applications as nanoreactor, as artificial organelles, or as drug-delivery devices require an exchange of substances between the outside and the inside of polymersomes. Here, a simple and versatile method is presented to render polymersomes semipermeable. It does not require complex membrane proteins or pose requirements on the chemical nature of the polymers. Vesicles made from three different amphiphilic block copolymers (*α*,*ω*-hydroxy-end-capped poly(2-methyl-2-oxazoline)-*block*-poly(dimethylsiloxane)-*block*-poly(2-methyl-2-oxazoline) (PMOXA-*b*-PDMS-*b*-PMOXA), *α*,*ω*-acrylate-end-capped PMOXA-*b*-PDMS-*b*-PMOXA, and poly(ethylene oxide)-*block*-poly(butadiene) (PEO-*b*-PB)) were reacted with externally added 2-hydroxy-4′-2-(hydroxyethoxy)-2-methylpropiophenone under UV-irradiation. The photoreactive compound incorporated into the block copolymer membranes independently of their chemical nature or the presence of double bonds. This treatment of polymersomes resulted in substantial increase in permeability for organic compounds while not disturbing the size and the shape of the vesicles. Permeability was assessed by encapsulating horseradish peroxidase into vesicles and measuring the accessibility of substrates to the enzyme. The permeability of photoreacted polymersomes for ABTS, AEC, pyrogallol, and TMB was determined to be between 1.9 and 38.2 nm s^{-1}. It correlated with the hydrophobicity of the compounds. Moreover, fluorescent dyes were released at higher rates from permeabilized polymersomes compared to unmodified ones. The permeabilized nanoreactors retained their ability to protect encapsulated biocatalysts from degradation by proteases.

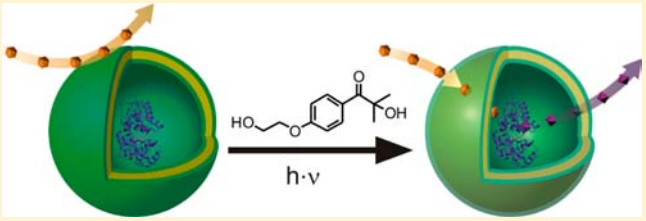

INTRODUCTION

Some amphiphilic block copolymers self-assemble in aqueous solution into vesicles, also called polymersomes. These nanocapsules enclose a pool of water that is delimitated by a membrane similar to the lipid bilayer membrane in liposomes and living cells. Compared to their lipid-based counterparts, block copolymer membranes are more stable and therefore more robust against, e.g., mechanical shear forces or disassembly upon dilution.[1] Moreover, their surface functionality, the chemical properties of the membrane, and its thickness can easily be tailored through the synthesis of the polymers.[2,3] Thus, block copolymer vesicles have gathered much interest as drug-delivery vehicles in nanomedicine, for *in vivo* imaging purposes, or as artificial organelles.[1,4,5] When catalytically active guests are encapsulated within the inner compartment of polymersomes, they can be used as nanoscale reactor vessels, i.e., as nanoreactors.[5−8] Within the confined space provided by the vesicle, reactions can occur with higher selectivity or less side reactions.[9] Furthermore, reactions and proteins can be monitored on the single molecule level using nanoreactors.[10,11] Cascade reactions of two or more catalytic species become more efficient due to the close spatial proximity and precise positioning of the catalysts.[12−14] Apart from confining reactions into nanoscale volumes, nanoreactors also protect the encapsulated guest from degrading agents and enzymes outside of the vesicles.[15] This is especially important for biomedical applications of nanoreactors, where an encapsulated enzyme produces a drug or scavenges toxic substances in intra- or extracellular fluids.[1,5,14,16] The physical and chemical stability of polymeric vesicles is of great importance for nanoreactor applications. However, the main advantage of the polymersomes is at the same time a disadvantage due to the difficulty to exchange substances between the interior and the exterior through the polymer membrane barrier.[17] A molecule entering or leaving a

Received: April 26, 2013
Published: May 24, 2013

dx.doi.org/10.1021/ja404175x | J. Am. Chem. Soc. 2013, 135, 9204−9212

polymersome would have to permeate a hydrophilic, a hydrophobic, and again an hydrophilic layer of membrane. With an increase in the molecular weight of the molecules that form the membrane of vesicles, it becomes less permeable.[3] While liposomes are permeable for cations and small molecules (e.g., glycerol, urea, ethylene glycol),[18] the shell of most polymersomes is virtually impermeable to small hydrophilic molecules but is permeable to gases.[19,20] For example, water, calcium ions, and many organic molecules cannot permeate through the membrane of the well-studied poly(2-methyl-2-oxazoline)-*block*-poly(dimethylsiloxane)-*block*-poly(2-methyl-2-oxazoline) (PMOXA-*b*-PDMS-*b*-PMOXA) block copolymer vesicles.[21−23] However, for chemical reactions to take place inside of nanoreactors, substrates must be able to enter the interior of the polymersomes, e.g., by diffusion through the membrane or through pores in the membrane. Also, most other applications of polymersomes require at some point the diffusion of small molecules toward the inner confined space or a release of content from the polymersomes.[4,6,8]

The permeability of polymersomes can be enhanced by using organic cosolvents.[24] Some block copolymers, such as poly(styrene)-*block*-polyisocyanoalanine(2-thiophene-3-yl-ethyl)-amide, form intrinsically porous membranes that allow free passage of small organic molecules.[15,25] Other permeable polymersomes are based on copolypeptides[26] or boronic acid-based block copolymers.[27] The permeability of polymersomes can be tuned by using photocross-linkable block copolymers that contain photocross-linkers as monomers in their hydrophobic block.[28−30] Another approach was explored by Meier and co-workers, who reconstituted channel proteins (e.g., OmpF, aquaporins) within membranes of PMOXA-*b*-PDMS-*b*-PMOXA copolymers.[5,21−23,31] Channel proteins render the polymersomes permeable to those molecules that can pass through the porins and therefore enable the effective design of nanoreactors.[4,6] All these approaches can only be applied in particular cases and are not very versatile. They either require the synthesis of special polymer blocks or need membrane proteins that are difficult to handle and expensive.

Here we present a simple, adaptable and easy-to-use method of introducing permeability into polymersomes. An α-hydroxyalkylphenone, 2-hydroxy-4′-2-(hydroxyethoxy)-2-methylpropiophenone (PP-OH), was added to solutions of polymeric vesicles and was allowed to react with the polymer membranes under UV-irradiation. This type I photoninitiator is water-soluble.[32] UV-irradiation causes it to form two primary radicals (ketyl and alcohol).[33] In its common application, these radicals would start a radical polymerization. However, in the absence of monomers, the radicals can recombine or attack other organic compounds,[33] similar to the well-studied benzophenone derivatives.[34] In our case, the radicals react with block copolymers in the polymersome membranes, causing chemical modification of the polymers with the hydrophilic PP-OH and therefore increase the permeability of the membranes toward hydrophilic molecules. The concentration of PP-OH was low enough to avoid cross-linking reactions between polymer chains. In order to explore the versatility of this permeabilization method, we chose three block copolymers that form vesicles but differ in their chemical properties: an α,ω-hydroxy-terminated PMOXA-*b*-PDMS-*b*-PMOXA block copolymer, an α,ω-acrylate-end-functionalized PMOXA-*b*-PDMS-*b*-PMOXA (A-PMOXA-*b*-PDMS-*b*-PMOXA-A), and a poly(ethylene oxide)-*block*-poly(butadiene) with a carboxylic acid end group (PEO-*b*-PB) (see Chart S1 for structures). While the first polymer does not bear any functional group that specifically reacts with radicals, the two latter polymers contain double bonds at the chain ends or in the PB block, respectively. These polymers are prone to be attacked by radicals and could potentially undergo cross-linking reactions in the presence of radicals. However, under the chosen reaction conditions, attachment of PP-OH to the polymer chains is favored over cross-linking reactions (*vide infra*).

Polymersomes that encapsulated the enzyme horseradish peroxidase (HRP) were used to show that permeability can be induced by photoreaction with PP-OH. To this end, access of various chromogenic substrates from the outside of such nanoreactors to the encapsulated biocatalysts was monitored, and the permeability correlated to structural features of the substrates. HRP is a 44 kDa heme enzyme that uses hydrogen peroxide to oxidize electron-rich aromatic compounds.[35,36] It finds applications in immunoassays, as a catalyst for biotransformations, in wastewater treatment, and as a polymerization catalyst.[36−39]

As a second method to prove the increase in membrane permeability upon PP-OH treatment, fluorescent dyes were encapsulated in self-quenching concentrations into the polymersomes, and the release of the dyes from the permeabilized polymersomes was measured.

RESULTS AND DISCUSSIONS

Morphology and Dimensions of Empty and HRP-Loaded Polymersomes. Polymersomes were generated by self-assembly of A-PMOXA-*b*-PDMS-*b*-PMOXA-A, PMOXA-*b*-PDMS-*b*-PMOXA, and PEO-*b*-PB, using the film rehydration method in phosphate buffer at pH 6.5.[40] In order to encapsulate HRP, film rehydration was carried out in an aqueous solutions of this biomolecule. The loaded vesicles were purified by size exclusion chromatography to remove non-encapsulated enzyme. The final concentration of encapsulated HRP into the polymersomes was quantified by UV−vis spectroscopy. The total concentration varied from 5.4 μM for HRP encapsulated in A-PMOXA-*b*-PDMS-*b*-PMOXA-A vesicles, to 18.6 μM for PMOXA-*b*-PDMS-*b*-PMOXA vesicles, and to 3.45 μM for PEO-*b*-PB vesicles.

The morphology and size of self-assembled structures were characterized by TEM and LS. In the absence of encapsulated HRP, TEM micrographs of A-PMOXA-*b*-PDMS-*b*-PMOXA-A show spherical structures with diameters ranging from 80 to 160 nm (Figures S1a). Similar structures with diameters of ∼90 nm were obtained with PMOXA-*b*-PDMS-*b*-PMOXA (Figure S1b), while TEM of self-assembled PEO-*b*-PB revealed tubular structures (Figure S1c). Light-scattering allows measuring the radii of gyration (R_g) and the hydrodynamic radius (R_h) of the self-assembled objects (Table 1). The ratio R_g/R_h (ρ-parameter) then reveals the morphology of the structures. The objects formed by A-PMOXA-*b*-PDMS-*b*-PMOXA-A have an average R_g of 127 nm, for PMOXA-*b*-PDMS-*b*-PMOXA present an average R_g of 108 nm, while PEO-*b*-PB forms much larger structures that could not be extruded through a 200 nm filter. ρ was 0.96 for A-PMOXA-*b*-PDMS-*b*-PMOXA-A, and 1.04 for PMOXA-*b*-PDMS-*b*-PMOXA. These values are close to the theoretical ρ of hollow spheres (1.0), indicating the presence of vesicles.[41,42] For PEO-*b*-PB a ρ-parameter of 1.3 was measured, which shows that the sample contained worm-like structures.[42]

dx.doi.org/10.1021/ja404175x | J. Am. Chem. Soc. 2013, 135, 9204−9212

Table 1. LS Data for Polymersomes and Self-Assembled Nanostructures

system	R_g, nm	R_h, nm	$\rho = R_g/R_h$
A-PMOXA-*b*-PDMS-*b*-PMOXA-A[a]	127	131	0.96
A-PMOXA-*b*-PDMS-*b*-PMOXA-A-HRP[b]	162	173	0.93
A-PMOXA-*b*-PDMS-*b*-PMOXA-A-HRP-PP-OH[c]	151	158	0.95
PMOXA-*b*-PDMS-*b*-PMOXA[a]	108	103	1.04
PMOXA-*b*-PDMS-*b*-PMOXA-HRP[b]	119	121	0.98
PMOXA-*b*-PDMS-*b*-PMOXA-HRP-PP-OH[c]	124	137	0.90
PEO-*b*-PB[a]	576	443	1.3
PEO-*b*-PB-HRP[b]	147	165	0.89
PEO-*b*-PB-HRP-PP-OH[c]	127	131	0.96

[a]Self-assembled in the absence of enzyme. [b]Self-assembled in the presence of HRP. [c]Self-assembled in the presence of HRP and photoreacted with 1 mg mL^{-1} PP-OH.

In the presence of HRP, all three copolymers formed spherical structures with diameters ranging from 50 to 240 nm, as visualized by TEM (Figure 1). No worm-like micelles or giant vesicles were observed in the case of PEO-*b*-PB copolymers. R_g was determined to be 162 nm for A-PMOXA-*b*-PDMS-*b*-PMOXA-A, 119 nm for PMOXA-*b*-PDMS-*b*-PMOXA, and 147 nm for PEO-*b*-PB (Table 1). In all cases, ρ was slightly below 1.0. The combination of LS and TEM data indicates that, when hydrated in the presence of HRP, the three copolymers self-assemble into polymersomes. The difference in self-assembling behavior of PEO-*b*-PB in the absence and the presence of the enzyme indicate that the guest induces vesicle formation.

Photoreactions within the Polymersome Membrane. Polymersomes were photoreacted with PP-OH in order to increase their permeability. To this end, PP-OH was added to solutions of polymersomes. Oxygen could interfere with the radicals that form upon activation of PP-OH. Thus, the mixtures were purged with argon. Then they were irradiated for 30 s with an UV-A lamp and purified by size-exclusion chromatography.

In a first set of experiments the optimal concentration of PP-OH was determined with HRP-loaded A-PMOXA-*b*-PDMS-*b*-PMOXA-A polymersomes. Vesicles of the acrylate-end-capped block copolymer were chosen, as they are most susceptible to cross-linking reactions that could interfere with the permeabilization. The concentration of PP-OH was varied between 0.1 and 5 mg mL^{-1}. PP-OH concentrations up to 1 mg mL^{-1} did not disturb the size and morphology of HRP-loaded vesicles (Figure S2). Exemplarily, the results for vesicles reacted with 1 mg mL^{-1} PP-OH are reported in Figure 1 and in Table 1. Spherical structures similar in size to those of HRP-loaded vesicles prior to PP-OH treatment were detected by TEM and LS. The ρ-parameters indicate that these objects are vesicles. Higher concentrations of the photoactive compound during UV-irradiation decreased the size of the polymersomes, as determined by TEM (Figure S2). Vesicles with an average diameter of 200 nm were obtained at a PP-OH concentration of 1.1 mg mL^{-1}. A PP-OH concentration of 1.5 mg mL^{-1} resulted in vesicles with a diameter of ~70 nm and micelles. Higher PP-OH concentrations lead to the aggregation of the polymers: At a PP-OH concentration of 2 mg mL^{-1}, almost no nanostructures were visible in TEM images (except for micelles), and at concentrations of 2.5 mg mL^{-1} or above, no self-assembled structures could be detected in TEM, probably due to inter- and intravesicle cross-linking. PP-OH concentrations below 1 mg mL^{-1} PP-OH did not render the vesicles permeable, as determined by the 2,2′-azino-bis(3-ethylbenzothiazoline-6-sulfonic acid) (ABTS) assay for encapsulated HRP (data not shown). A concentration of 1 mg mL^{-1} PP-OH, however, resulted in a substantial increase in permeability of the vesicles. These findings will be reported in detail below. Concluding, a PP-OH concentration of 1 mg mL^{-1} resulted in permeable vesicles with undisturbed size. Therefore, this PP-OH concentration was chosen for all further experiments.

Photoreaction of PP-OH with polymersomes should result in the incorporation of the photoreactive compound into the polymersome membrane. Thus, it was investigated by UV−vis spectroscopy if size exclusion chromatography (SEC)-purified vesicles showed the absorption band that is characteristic to PP-OH and its derivatives. Figure 2 compares UV−vis spectra of HRP-loaded A-PMOXA-*b*-PDMS-*b*-PMOXA-A, PMOXA-*b*-PDMS-*b*-PMOXA, and PEO-*b*-PB polymersomes before and after PP-OH treatment. The spectra of the photoreacted vesicles show an absorption band with a maximum at 280 nm. It is absent in the spectra of the vesicles that were not treated with PP-OH. This band can be attributed to the hydroxyethoxy phenyl ketone, as similar spectra were reported for PP-OH and

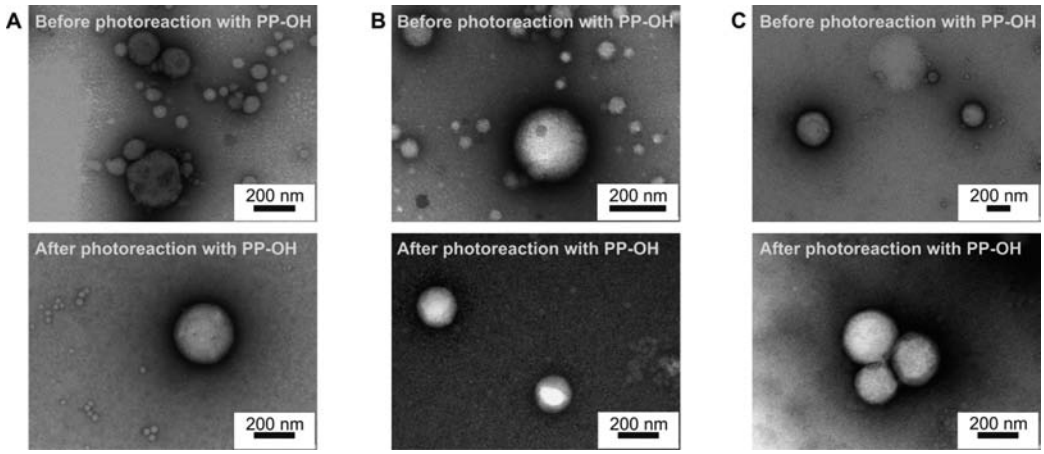

Figure 1. TEM micrographs of HRP-filled polymersomes before and after photoreaction with PP-OH. (A) A-PMOXA-*b*-PDMS-*b*-PMOXA-A, (B) PMOXA-*b*-PDMS-*b*-PMOXA, and (C) PEO-*b*-PB.

dx.doi.org/10.1021/ja404175x | J. Am. Chem. Soc. 2013, 135, 9204−9212

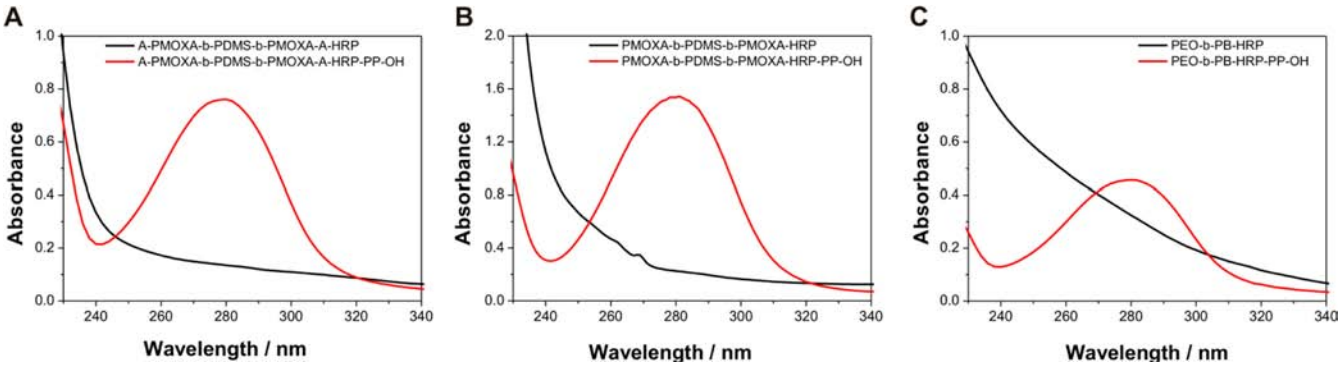

Figure 2. UV spectra of HRP-loaded polymersomes before and after photoreaction with PP-OH. (A) A-PMOXA-*b*-PDMS-*b*-PMOXA-A, (B) PMOXA-*b*-PDMS-*b*-PMOXA, and (C) PEO-*b*-PB. All samples were purified by SEC prior to recording of the spectra in order to remove small molecules that are not bound to the polymersomes.

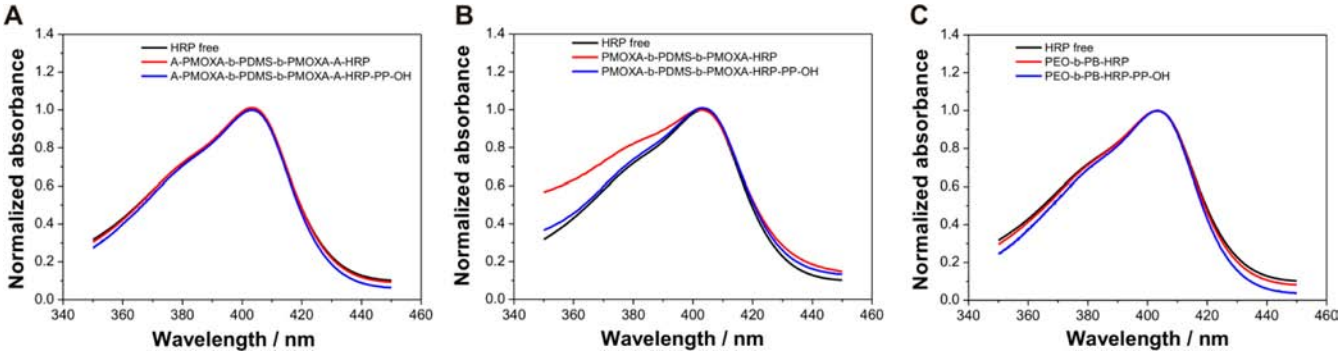

Figure 3. Normalized UV−vis spectra of free HRP and of HRP in polymersomes before and after photoreaction with PP-OH. (A) A-PMOXA-*b*-PDMS-*b*-PMOXA-A, (B) PMOXA-*b*-PDMS-*b*-PMOXA, and (C) PEO-*b*-PB. The spectra were normalized to 1 at maximal absorbance in order to facilitate the comparison of the spectra.

some of its derivatives in the literature (e.g., the absorption maximum of PP-OH in acetonitrile is at 276 nm).[43] The UV−vis data were complemented by gel permeation chromatography (GPC) of the polymers. A number-average molecular weight (M_n) of 6000 g mol^{-1} was measured for A-PMOXA-*b*-PDMS-*b*-PMOXA-A. PP-OH-treated vesicles were disrupted by solvent exchange to THF and then analyzed by GPC. A-PMOXA-*b*-PDMS-*b*-PMOXA-A now had a M_n of 7230 g mol^{-1}. Similar results were obtained for PEO-*b*-PB (4900 g mol^{-1} before and 6400 g mol^{-1} after PP-OH treatment). These results indicate that no cross-linking occurred upon photoreaction of the double-bond bearing polymersomes with PP-OH, as it would have led to a much higher increase in molecular weight. Instead, the slightly increased M_n can be explained by the attachment of small molecules to the polymers. Possibly, the reaction of PP-OH with the polymersomes increases the hydrophilicity of the membrane and therefore renders it permeable for hydrophilic substances.

Encapsulation Efficiency. In order to determine if the heme protein is stable under the photoreaction conditions and whether the reaction has an effect on the encapsulation efficiency of the enzyme, UV−vis spectra of encapsulated HRP were recorded before and after PP-OH treatment and compared to the spectrum of nonencapsulated, native HRP (Figure 3). All spectra show HRP's characteristic Soret band with a maximum at 403 nm,[35,44] indicating that the enzyme's active site was not modified by PP-OH. UV−vis spectra also allow quantifying the concentration of HRP. In the A-PMOXA-*b*-PDMS-*b*-PMOXA-A-PP-OH system the enzyme's concentration was 2.5 μM (0.12 mg mL^{-1}), in the solution of PMOXA-*b*-PDMS-*b*-PMOXA-PP-OH vesicles it was 17 μM, and with PEO-*b*-PB-PP-OH vesicles it was 2.6 μM. Therefore, the concentration of HRP in the PMOXA-*b*-PDMS-*b*-PMOXA-based vesicles did only decrease slightly upon photoreaction with PP-OH. The double-bond containing polymersomes, however, lost between 54% (A-PMOXA-*b*-PDMS-*b*-PMOXA-A) and 25% (PEO-*b*-PB) of their enzyme load. Most likely, the additional purification step by SEC removed some aggregated vesicles as well as enzyme released from polymersomes during the reaction with PP-OH. Nevertheless, sufficient amounts of the peroxidase were retained in all types of vesicles upon PP-OH treatment to allow for permeability measurements and to use the PP-OH treated vesicles as nanoreactors for biotransformations.

Permeability Studies in the PP-OH-Treated Polymersomes. The changes in membrane permeability of polymersomes upon PP-OH treatment were investigated by kinetic assays of the encapsulated HRP. To this end, HRP-filled vesicles were exposed to solutions of hydrogen peroxide and four different chromogenic HRP substrates: ABTS,[45,46] 3-amino-9-ethyl carbazole (AEC),[47] pyrogallol,[48] and 3,3′,5,5′-tetramethylbenzidine (TMB)[49] (Chart 1). These four substrates were chosen because they are all small organic molecules, but they differ in their hydrophilicity. This is expressed by their solubility in water. It ranges from 0.1 g L^{-1} for AEC to 400 g L^{-1} for pyrogallol (Table 2).[50−53] Thus, a correlation between their hydrophilicity and their ability to diffuse into PP-OH-treated vesicles might be possible. All substrates are converted by the enzyme into colored products, so that these reactions can be monitored by UV−vis

dx.doi.org/10.1021/ja404175x | J. Am. Chem. Soc. 2013, 135, 9204−9212

Chart 1. HRP Substrates Used in Permeability Studies

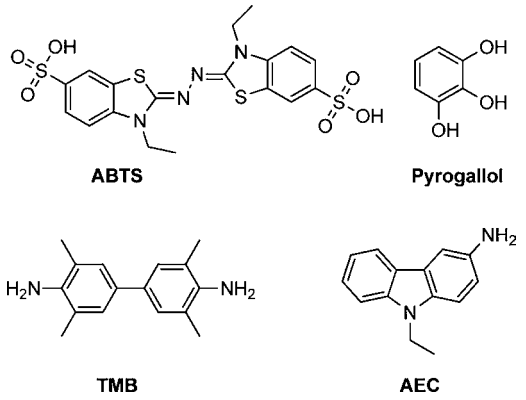

Table 2. Permeability of PP-OH-Treated Polymersomes for HRP Substrates

substrate	solubility of substrate in water at 20 °C/g·L	polymersome	permeability, nm·s^{-1}
pyrogallol	400[a]	A-PMOXA-*b*-PDMS-*b*-PMOXA-A-HRP-PP-OH	12.2 ± 0.6
		PMOXA-*b*-PDMS-*b*-PMOXA-HRP-PP-OH	3.03 ± 0.2
		PEO-*b*-PB-HRP-PP-OH	1.9 ± 0.02
ABTS	20[b]	A-PMOXA-*b*-PDMS-*b*-PMOXA-A-HRP-PP-OH	14.4 ± 0.7
		PMOXA-*b*-PDMS-*b*-PMOXA-HRP-PP-OH	8.07 ± 0.1
		PEO-*b*-PB-HRP-PP-OH	3.5 ± 0.2
TMB	1[c]	A-PMOXA-*b*-PDMS-*b*-PMOXA-A-HRP-PP-OH	20.8 ± 0.2
		PMOXA-*b*-PDMS-*b*-PMOXA-HRP-PP-OH	18.9 ± 0.8
		PEO-*b*-PB-HRP-PP-OH	14.7 ± 0.3
AEC	0.1[d]	A-PMOXA-*b*-PDMS-*b*-PMOXA-A-HRP-PP-OH	32.4 ± 0.6
		PMOXA-*b*-PDMS-*b*-PMOXA-HRP-PP-OH	38.2 ± 0.9
		PEO-*b*-PB-HRP-PP-OH	27.1 ± 0.09

[a]Ref 50. [b]Ref 51. [c]Ref 52. [d]Ref 53.

spectroscopy. As the HRP-catalyzed oxidation reactions are fast (e.g., for ABTS a rate constant of 8×10^8 M^{-1} s^{-1} has been reported[54]), a calculation method to determine permeabilities of polymersomes introduced by Battaglia and Ryan can be employed.[55]

HRP catalyzes a one-electron oxidation of ABTS to yield a metastable radical cation with blue-green color.[45,46] As expected, the reaction with free HRP resulted in an increase in absorbance at 414 nm over time (Figure 4). In contrast, HRP encapsulated in A-PMOXA-*b*-PDMS-*b*-PMOXA-A, PMOXA-*b*-PDMS-*b*-PMOXA, and PEO-*b*-PB vesicles gave no colorimetric reaction within at least 50 min. However, when PP-OH-treated vesicles were used, the substrate was converted to its colored form, and absorbance at 414 nm increased. In control reactions it was ruled out that PP-OH in the membrane catalyzes the conversion of the substrates. Activity assays with empty, PP-OH-treated PMOXA-*b*-PDMS-*b*-PMOXA vesicles did not develop color (Figure S3). Furthermore, it was tested whether UV-irradiation was necessary to induce permeability with PP-OH, or if a mere dissolution of PP-OH in the membrane was

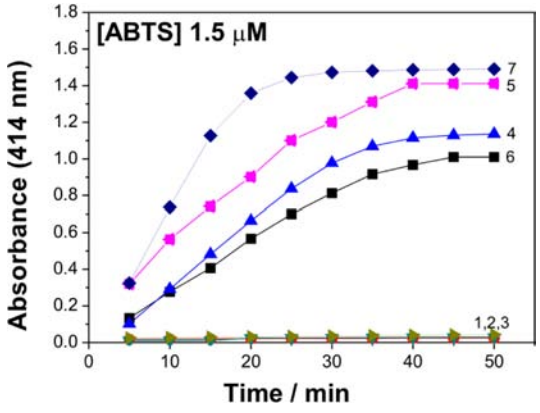

Figure 4. HRP activity assays with ABTS as substrate to determine the increase in polymersome permeability upon photoreaction with PP-OH. (1–3) HRP-filled polymersomes before photoreaction with PP-OH. (4–6) HRP-filled polymersomes after photoreaction with PP-OH: (4) A-PMOXA-*b*-PDMS-*b*-PMOXA-A-HRP-PP-OH, (5) PMOXA-*b*-PDMS-*b*-PMOXA-HRP-PP-OH, (6) PEO-*b*-PB-HRP-PP-OH. (7) Free HRP. The initial slope of such kinetic measurements was used to calculate permeabilities.

enough to render the polymersomes permeable. To this end, HRP-filled PMOXA-*b*-PDMS-*b*-PMOXA vesicles were incubated with PP-OH but not irradiated. Activity assays with these vesicles did not show any color formation (Figure S3). These findings allow concluding that the enzyme was active inside of the polymersomes and that the substrate was only able to access HRP when the vesicles had been photoreacted with PP-OH. Thus, the light-induced reaction of the α-hydroxyalkylphenone with A-PMOXA-*b*-PDMS-*b*-PMOXA-A, PMOXA-*b*-PDMS-*b*-PMOXA, and PEO-*b*-PB rendered the vesicles permeable for the HRP substrate. Similar results were obtained for AEC, pyrogallol, and TMB (Figure S3), and the permeabilization results for all four substrates are summarized in Table 2. Permeability for ABTS across the PP-OH-modified block copolymer membranes was calculated to be 14.4 nm s^{-1} (A-PMOXA-*b*-PDMS-*b*-PMOXA-A-PP-OH), 8.07 nm s^{-1} (PMOXA-*b*-PDMS-*b*-PMOXA), and 3.5 nm s^{-1} (PEO-*b*-PB-PP-OH), respectively. The permeability of PP-OH-treated polymersomes toward the more hydrophobic substrate TMB is 1.4- to 4.2-times higher. AEC, the most hydrophobic compound of the four tested ones, permeates the polymersome membranes 2.3- to 23.6-fold better than ABTS. On the other hand, the permeability of the polymersomes to the much more hydrophilic pyrogallol is significantly lower than the values determined for ABTS, TMB, or AEC. Thus, these four compounds diffuse more easily through the blockcopolymer membranes the more hydrophobic they are.

Protection of Encapsulated Enzyme against an Externally Added Degrading Agent. Many of the experimental results presented above, including the coelution of enzyme and polymersomes in the same fraction of size exclusion chromatography, and the accessibility of externally added substrates to the biocatalyst, indicate that PP-OH-treated polymersomes encapsulated HRP in their inside. However, a second scenario cannot be ruled out completely by these experiments. PP-OH treatment could result in the release of enzyme from some of the polymersomes, followed by an attachment or adsorption of the HRP to the outside of intact vesicles. This would challenge our hypothesis that the UV-induced reaction of PP-OH with polymersomes causes an

dx.doi.org/10.1021/ja404175x | J. Am. Chem. Soc. 2013, 135, 9204–9212

increase in membrane permeability. Thus, control experiments were carried out in which proteinase K was added to solutions of HRP-loaded and PP-OH-treated A-PMOXA-*b*-PDMS-*b*-PMOXA-A polymersomes as well as to solutions of free HRP. The rationale of these experiments is that the protease digests and deactivates all HRP that is accessible from the external aqueous phase, while HRP that resides inside of polymersomes is protected against proteolytic attack and therefore retains its activity. After incubation at 40 °C for 24 h, activity assays with ABTS were carried out. Apparent activities were determined from initial slopes in absorbance vs time plots. Figure 5 shows the results of such digestion

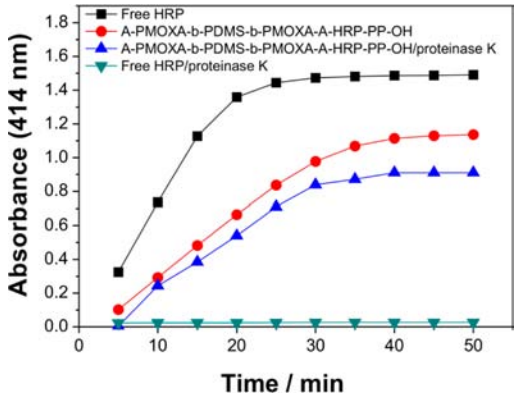

Figure 5. Protection of HRP in PP-OH-treated A-PMOXA-*b*-PDMS-*b*-PMOXA-A polymersomes against an externally added protease. Samples of free HRP and of encapsulated HRP were incubated for 24 h at 40 °C in a solution of proteinase K. Then, the activity of HRP was probed with the ABTS assay. For comparison, kinetic runs of samples without proteinase K digestion are also shown.

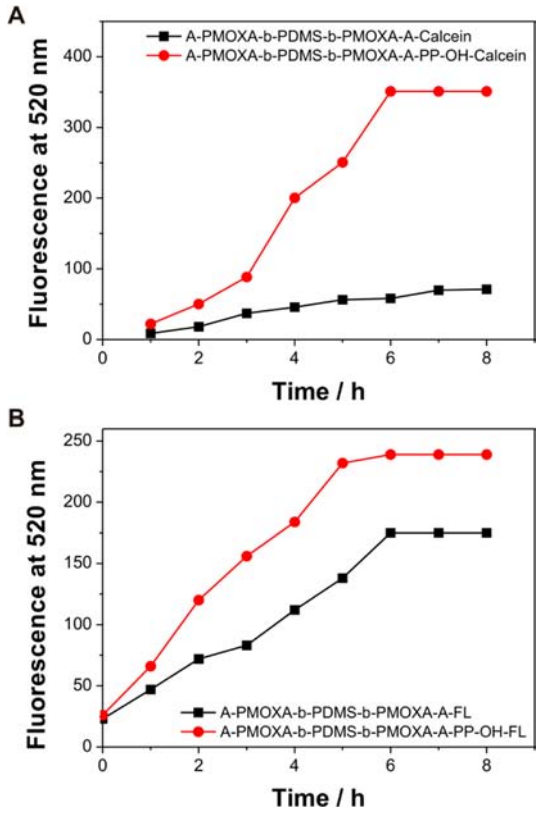

Figure 6. Release of fluorescent dyes from A-PMOXA-*b*-PDMS-*b*-PMOXA-A polymersomes and from PP−OH-treated A-PMOXA-*b*-PDMS-*b*-PMOXA-A polymersomes. A) Increase in calcein fluorescence at 520 nm over time. B) Increase in fluorescein (FL) fluorescence at 520 nm over time.

experiments. For comparison, the activity assays of samples that were not treated with the protease are also shown. The peroxidase in the PP-OH-treated vesicles retained 80% of its activity. In contrast, enzymatic digestion of free HRP resulted in a complete deactivation of the enzyme. These results confirm that HRP is encapsulated in the PP-OH-treated polymersomes and show that the polymersomes have the ability to protect the enzyme from the digestive action of the protease. Thus, the PP-OH-modified polymer membrane is semipermeable for small organic molecules, while the investigated biomacromolecules are too large to cross the membrane of the vesicles.

Release Kinetics of Low Molecular Weight Molecules. In the previous paragraphs we have shown that UV-induced modification of polymersomes with PP-OH allows organic molecules to penetrate the block copolymer polymer membrane from the external aqueous phase into the vesicles. However, the flux of molecules in the reverse direction, from the inside of vesicles into the solution medium, is essential for many applications, ranging from drug-producing nanoreactors to controlled release drug-delivery systems. In order to test the ability of polymersomes to release a molecular cargo upon treatment with PP-OH, two fluorescent dyes, calcein and fluorescein, were encapsulated into A-PMOXA-*b*-PDMS-*b*-PMOXA-A polymersomes in concentrations high enough to induce self-quenching of fluorescence. Release of dye from the polymersome into solution causes dilution of the dye and therefore an increase in fluorescence intensity, so that the release kinetics can be followed by fluorescence spectroscopy. Figures 6 and S4 show the results of calcein release from A-PMOXA-*b*-PDMS-*b*-PMOXA-A vesicles. The nonmodified vesicles only caused a minor increase in fluorescence emission over time, indicating a slow leakage of the dye from the polymersomes. However, when the vesicles were reacted with PP-OH prior to the release experiment, the initial rate of fluorescence increase was significantly higher. After 6 h, the fluorescence stayed constant. Thus, PP-OH enhanced the permeability of the block copolymer membrane toward calcein, and the dye could diffuse at a higher rate out of the polymersomes, until equilibrium of dye concentration inside and outside of the polymersome was reached at 6 h. Similar observations were made for the release of the second dye, fluorescein, from A-PMOXA-*b*-PDMS-*b*-PMOXA-A vesicles (Figures 6 and S4). Reaction of PP-OH with the polymersomes resulted in the dye diffusing out of the polymersomes at a higher rate compared to polymersomes that were not reacted with the photoactive compound. However, the difference in release rate is less pronounced than in the case of calcein, due to the fact that vesicles that were not treated with PP-OH are already considerable leaky for fluorescein under the tested conditions at pH 6.5. The latter result is in agreement with the finding that fluorescein is able to cross amphiphilic bilayer membranes, such as artificial lipid membranes at this pH.[56]

■ CONCLUSIONS

Photoreaction of PP-OH with polymersomes is a versatile way to induce permeability in polymer vesicles. The permeabilization method was successfully tested with three different block copolymers (A-PMOXA-*b*-PDMS-*b*-PMOXA-A, PMOXA-*b*-

dx.doi.org/10.1021/ja404175x | *J. Am. Chem. Soc.* 2013, 135, 9204−9212

PDMS-*b*-PMOXA, and PEO-*b*-PB) and proved to be independent of the presence of specific functional groups. This suggests a broad applicability of the method. At a PP-OH concentration of 1 mg mL^{-1} neither the morphology, the size, nor the stability of the polymeric vesicles is affected by the photoreaction. The modification of the polymers with PP-OH resulted in a selective permeability of the membranes for various small organic compounds, while keeping the ability of the polymersomes to retain an enzyme in their interior. Therefore, photoreaction with PP-OH is a well-suited method to turn enzyme-filled polymersomes into nanoreactors without the need of membrane proteins or specially designed polymer blocks. Modification with PP-OH does not affect the ability of the nanoreactors to protect the encapsulated biocatalyst against denaturating agents outside of the vesicle. This was demonstrated by incubation with a protease, which, under similar conditions, induced the inactivation of free HRP. Permeability of nanoreactors for various substrates was between 1.9 and 32.4 nm s^{-1} and depends upon the hydrophobicity of the compounds. To put these numbers into perspective, it is useful to compare them to the permeability of a compound known to easily permeate block copolymer membranes due to its less hydrophilic character: 5,5′-dithiobis(2-nitrobenzoic acid) has a permeability across poly(ethylene oxide)-*b*-poly(butylene oxide) block copolymer vesicle membranes of 0.43 nm s^{-1}.[40] Thus, the PP-OH induced permeability in the tested PMOXA-*b*-PDMS-*b*-PMOXA and PEO-*b*-PB polymersomes is rather high. Photoreaction of polymersomes with PP-OH does not only yield nanoreactors but is also a useful method to increase the release rate of encapsulated organic compounds from vesicles, allowing the slow diffusion of low molecular weight compounds out of polymersomes for up to six hours. This in turn could lead to novel controlled release systems, e.g., for drug delivery.

EXPERIMENTAL SECTION

Materials. A-PMOXA-*b*-PDMS-*b*-PMOXA-A; M_n = 6000 g mol^{-1}, polydispersity index (PDI) = 1.2 (determined by GPC), ratio MOXA:DMS:MOXA 14:33:14 (determined by ^{1}H NMR) was purchased from Polymer Source (Quebec) and used as received. PMOXA-*b*-PDMS-*b*-PMOXA; M_n = 4500 g mol^{-1}, PDI = 1.4 (determined by GPC), ratio MOXA:DMS:MOXA 5:20:5 (determined by ^{1}H NMR) was synthesized according to a previously published protocol.[57] The synthesis of poly(ethylene oxide)-*block*-poly(butadiene) bearing a succinic acid group at the PEO chain end (PEO-*b*-PB; M_n = 4900 g mol^{-1}, PDI = 1.12 (determined by GPC), ratio of EO:B of 34:60 (determined by ^{1}H NMR)) was described elsewhere.[58] Fluorescein, calcein, HRP (highly stabilized, essentially salt-free, lyophilized powder, 200−300 units/mg solid), PP-OH (also known as Irgacure 2959), AEC, ABTS, TMB (Elisa test kit), Sepharose 2B, and proteinase K were obtained from Sigma-Aldrich and used as is. Phosphate buffer (10 mM, pH 6.5, 136 mM NaCl, 2.6 mM KCl) was prepared by solving 8 g NaCl, 0.2 g KCl, 1.44 g Na_2HPO_4, and 0.24 g of KH_2PO_4 in 800 mL ddH_2O, adjusting the pH with HCl and completing the volume to 1 L.

Preparation of Polymersomes. Polymersomes were formed using the film rehydration method.[40] For this, a solution of polymer (4 mg mL^{-1}) in chloroform (1 mL) was slowly evaporated in a 5 mL round-bottom flask by means of a rotary vacuum evaporator at reduced pressure until the solvent evaporated completely and a film formed on the flask wall. In a second step, the polymer film was rehydrated under magnetic stirring for 12 h at room temperature with either: (1) 1 mL of phosphate buffer to form empty vesicles; (2) 1 mL of a solution of HRP (2 mg mL^{-1}) in phosphate buffer to form enzyme-loaded vesicles; or (3) 1 mL of a 100 mM solution of fluorescent dye (fluorescein or calcein) in phosphate buffer. The solutions were extruded through 200 nm polycarbonate filters (Whatman), and the polymersomes containing HRP were separated from the free enzyme by SEC using a Sepharose 2B column and phosphate buffer as mobile phase. In the case of polymersomes that encapsulated fluorescein or calcein, the samples were dialyzed overnight against 800 mL phosphate buffer, due to the high concentration of dye used for sample preparation, and purified thereafter by SEC as described above.

Photoreactions within the Polymersome Membrane. To 1 mL of loaded polymersomes, 0.1−5 mg PP-OH was added. The mixture was deoxygenated by bubbling with argon for 30 min and then irradiated for 30 s with UV light (315−405 nm) using a 400W UV flood lamp (UV Light Technology Limited, U.K.) fitted with an iron-doped metal halide UV bulb 230 V/50 Hz (Hamamatsu LC4) and a UV-A black filter glass. PP-OH-treated vesicles were separated from the free compound by SEC (Sepharose 2B, phosphate buffer as mobile phase) thereafter. For control experiments empty PMOXA-*b*-PDMS-*b*-PMOXA polymersomes were treated with 1 mg mL^{-1} PP-OH in oxygen free conditions and were subsequently UV-irradiated. Moreover, HRP- encapsulating PMOXA-*b*-PDMS-*b*-PMOXA polymersomes were treated with 1 mg mL^{-1} PP-OH in the same oxygen free conditions but were not UV irradiated in order to check the possible influence of the presence of unreacted PP-OH on the permeability.

Activity Assays of HRP and Determination of Polymersome Permeability. The permeability of the membrane of HRP-loaded vesicles was determined by means of activity assays for HRP using four different substrates (ABTS,[45,46] TMB,[49] AEC,[47] and pyrogallol[48]). To this end, the chromogenic substrates and hydrogen peroxide were added to an aqueous polymersome solution. The substrates have to permeate into the vesicles to be converted by the enzyme to colored products. The formation of these oxidized products was monitored by UV−vis spectroscopy. The ABTS assay was carried out at room temperature in 1 cm silica glass cuvettes by mixing 0.1 mL solution of the HRP-containing polymersomes with 0.5 mL aqueous ABTS solution (concentrations ranging from 0.2 to 6 μM) and 0.35 mL distilled H_2O. The reaction was started by the addition of 0.05 mL of 20 mM H_2O_2. Absorbance at 414 nm was recorded every 300 s.

Reference kinetic assays with nonencapsulated HRP were carried out in the same way, replacing the polymersome solution with 0.1 mL solution of HRP (0.2 mg mL^{-1}, 4.5 μM) in phosphate buffer.

The AEC and pyrogallol assays were carried out in way similar to the ABTS test, using 0.5 mL aqueous AEC solution (concentrations ranging from 22 to 46 nM), and 0.5 mL aqueous pyrogallol solution (concentrations ranging from 0.4 nM to 1.9 μM), respectively. Absorbance was monitored at 410 nm (AEC) or 420 nm (pyrogallol).

For the TMB assay, 0.1 mL free HRP or polymersomes that encapsulated HRP were mixed with 0.5 mL TMB-Elisa test solution (concentration 6.6−46%) and 0.4 mL H_2O. The reaction was started by the addition of 20 mM H_2O_2, and the increase in absorbance at 652 nm was measured over time.

First, a set of activity assays was carried out under variation of substrate concentration in the ranges stated above in order to determine at which concentrations the maximal velocity of substrate conversion V_{max} was achieved (V_{max} at c(ABTS) ≥ 1.5 μM, c(AEC) ≥ 11 nM, c(pyrogallol) ≥ 0.41 μM, c(TMB) ≥ 13%). Then, those kinetic assays that resulted in conversion rates up to V_{max} were selected to calculate permeabilities of substrates across vesicle membranes. To this end, a published equation was adapted.[55] From the initial linear increase of absorbance over time in these assays, the change of product concentration over time $dc(t)/dt$ was determined. In combination with the hydrodynamic diameter of the vesicles D (determined by DLS), the encapsulation efficiency of HRP e(HRP) defined as the ratio in between concentration of encapsulated HRP and HRP-concentration used for encapsulation (determined by UV−vis spectrometry), and the substrate concentration at t_{rxn} = 0 s ($c(\text{substrate})_0$), permeabilities p were calculated according to:

$$p = \frac{D}{6 \cdot e(\text{HRP}) \cdot c(\text{substrate})_0} \cdot \frac{dc(t)}{dt}$$

dx.doi.org/10.1021/ja404175x | J. Am. Chem. Soc. 2013, 135, 9204−9212

The mean values of five kinetic assays are reported. Error ranges are the standard deviations.

In control experiments the activities of empty PP-OH-treated PMOXA-*b*-PDMS-*b*-PMOXA polymersomes and of HRP-encapsulating PMOXA-*b*-PDMS-*b*-PMOXA polymersomes that were incubated with PP-OH but not irradiated were assessed using the maximal concentration of each substrate considered in our study.

Digestion of HRP with Proteinase K. 0.5 mL of a 200 μg mL^{-1} proteinase K solution in phosphate buffer was added to 0.5 mL sample solution (0.12 mg mL^{-1} HRP-filled vesicles treated with PP-OH or 2 mg mL^{-1} HRP solution) in 1 mL phosphate buffer. The reaction mixtures were incubated at 40 °C for 24 h. Then, the residual HRP activity was evaluated by the ABTS assay (with c(ABTS) = 1.5 μM) as described above. Activities were determined from the initial slope of absorbance vs time plots.

Release of Fluorescent Dyes from Vesicles. The vesicles were prepared in the presence of fluorescent dyes (fluorescein, calcein) and purified by SEC as described above. The release of dye from polymersomes that were not photoreacted with PP-OH was followed at room temperature by fluorescence spectroscopy (on a LS55 spectrometer, Perkin-Elmer). To this end, freshly purified polymersome solution (1.2 mg mL^{-1} in 5 mL phosphate buffer) was placed in a 1 cm quartz cuvette into the spectrometer and analyzed for 8 h in scan mode, taking emissions scans every hour with the excitation slit set to 10 nm and the emission slit set to 3 nm. The excitation wavelength was set to 494 nm, and the emission spectra were recorded from 500 to 650 nm. The release of dye from PP-OH-treated polymersomes was followed in the same way, using dye-loaded polymersomes that had been purified by size exclusion chromatography, photoreacted with PP-OH, and purified a second time by a SEC as detailed above.

Methods. The dimensions of the extruded vesicles were determined by dynamic and static light scattering (DLS, SLS). The measurements were performed on an ALV goniometer (Langen, Germany), equipped with an ALV He–Ne laser (λ = 632.8 nm) using serial dilutions to produce polymer concentrations ranging from 0.08 to 0.3 mg mL^{-1}. LS was measured in 10 mm cylindrical quartz cells at angles between 30 and 150° at 293 K. The photon intensity auto correlation function $g_2(t)$ was determined with an ALV-5000E correlator at scattering angles between 30° and 150°. The obtained data were processed using ALV static and dynamic fit and plot software (version 4.31 10/01). SLS data were processed according to the Guinier-model and DLS data by using a Williams–Watts function. The morphology as well the size of the formed polymersomes were characterized by TEM on a Philips EM400 electron microscope which was operated at 100 kV. Polymersome dispersions were deposited on a carbon-coated copper grid and negatively stained with 2% uranyl acetate solution. UV–vis spectroscopy was measured on a Specord 210 plus spectrometer (Analytik Jena, Jena, Germany) with a slit width of 4 nm in 1 cm quartz and silica glass cuvettes (Hellma). In order to determine HRP concentration in samples of enzyme-loaded polymersomes (with and without treatment with PP-OH) the Soret absorption at 403 nm was measured. An extinction coefficient of 0.9 × 10^5 M^{-1} cm^{-1} was used. It was determined experimentally with a dilution series of the enzyme in phosphate buffer. Gel permeation chromatography was used in order to determine the polymer's molecular weight variations induced by the reaction of polymersomes with PP-OH. M_n and PDI were determined using a Viscotek GPC max system equipped with four Agilent PLgel columns (10 μm guard; mixed C; 10 μm, 100 Å; 5 μm, 10^3 Å), using THF as eluent at a flow rate of 1 mL min^{-1} at 40 °C. Signals were recorded with a refractive-index detector and calibrated against polystyrene standards (Agilent).

■ ASSOCIATED CONTENT

Supporting Information

Structures of the polymers, additional TEM images, enzymatic activity assays, and fluorescence spectra. This material is available free of charge *via* the Internet at http://pubs.acs.org.

■ AUTHOR INFORMATION

Corresponding Author

nico.bruns@unibas.ch

Notes

The authors declare no competing financial interest.

M. S. is on scientific leave from the Institute of Macromolecular Chemistry "Petru Poni", 41A Grigore Ghica Voda, Iassy 74048, Romania.

■ ACKNOWLEDGMENTS

Generous financial support by the KTI/CTI, the Swiss National Science Foundation, the NCCR Nanosciences, the Marie-Curie-Actions of the European Commission, the Holcim Stiftung Wissen, and the University of Basel is gratefully acknowledged. The authors thank the Zentrum für Mikroskopie Basel (ZMB) for the TEM images, Sven Kasper and Gabriele Persy for experimental assistance, and Mark Inglin for editing the manuscript.

■ REFERENCES

(1) Brinkhuis, R. P.; Rutjes, F. P. J. T.; van Hest, J. C. M. *Polym. Chem.* **2011**, *2*, 1449–1462.

(2) Egli, S.; Schlaad, H.; Bruns, N.; Meier, W. *Polymers* **2011**, *3*, 252–280.

(3) Discher, D. E.; Eisenberg, A. *Science* **2002**, *297*, 967–973.

(4) Tanner, P.; Baumann, P.; Enea, R.; Onaca, O.; Palivan, C.; Meier, W. *Acc. Chem. Res.* **2011**, *44*, 1039–1049.

(5) Palivan, C. G.; Fischer-Onaca, O.; Delcea, M.; Itel, F.; Meier, W. *Chem. Soc. Rev.* **2012**, *41*, 2800–2823.

(6) Renggli, K.; Baumann, P.; Langowska, K.; Onaca, O.; Bruns, N.; Meier, W. *Adv. Funct. Mater.* **2011**, *21*, 1241–1259.

(7) Peters, R. J. R. W.; Louzao, I.; van Hest, J. C. M. *Chem. Sec.* **2012**, *3*, 335–342.

(8) Kim, K. T.; Meeuwissen, S. A.; Nolte, R. J. M.; van Hest, J. C. M. *Nanoscale* **2010**, *2*, 844–858.

(9) Vriezema, D. M.; Aragones, M. C.; Elemans, J. A. A. W.; Cornelissen, J. J. L. M.; Rowan, A. E.; Nolte, R. J. M. *Chem. Rev. (Washington, DC, U. S.)* **2005**, *105*, 1445–1489.

(10) Rosenkranz, T.; Katranidis, A.; Atta, D.; Gregor, I.; Enderlein, J.; Grzelakowski, M.; Rigler, P.; Meier, W.; Fitter, J. *ChemBioChem* **2009**, *10*, 702–709.

(11) Comellas-Aragones, M.; Engelkamp, H.; Claessen, V. I.; Sommerdijk, N. A. J. M.; Rowan, A. E.; Christianen, P. C. M.; Maan, J. C.; Verduin, B. J. M.; Cornelissen, J. J. L. M.; Nolte, R. J. M. *Nat. Nanotechnol.* **2007**, *2*, 635–639.

(12) van Dongen, S. F. M.; Nallani, M.; Cornelissen, J.; Nolte, R. J. M.; van Hest, J. C. M. *Chem.—Eur. J.* **2009**, *15*, 1107–1114.

(13) Vriezema, D. M.; Garcia, P. M. L.; Oltra, N. S.; Hatzakis, N. S.; Kuiper, S. M.; Nolte, R. J. M.; Rowan, A. E.; van Hest, J. C. M. *Angew. Chem., Int. Ed.* **2007**, *46*, 7378–7382.

(14) Tanner, P.; Onaca, O.; Balasubramanian, V.; Meier, W.; Palivan, C. G. *Chem.—Eur. J.* **2011**, *17*, 4552–4560.

(15) Kuiper, S. M.; Nallani, M.; Vriezema, D. M.; Cornelissen, J. J. L. M.; van Hest, J. C. M.; Nolte, R. J. M.; Rowan, A. E. *Org. Biomol. Chem.* **2008**, *6*, 4315–4318.

(16) Langowska, K.; Palivan, C. G.; Meier, W. *Chem. Commun. (Cambridge, U. K.)* **2013**, *49*, 128–130.

(17) Marguet, M.; Edembe, L.; Lecommandoux, S. *Angew. Chem., Int. Ed.* **2012**, *51*, 1173–1176.

(18) Peterlin, P.; Arrigler, V.; Diamant, H.; Haleva, E. In *Advances in Planar Lipid Bilayers and Liposomes*; Aleš, I., Ed.; Academic Press: New York, 2012; Vol. *16*, p 301–335.

(19) Montenegro, J.; Braun, J.; Fischer-Onaca, O.; Meier, W.; Matile, S. *Org. Biomol. Chem.* **2011**, *9*, 6623–6628.

(20) Piras, A. M.; Dessy, A.; Chiellini, F.; Chiellini, E.; Farina, C.; Ramelli, M.; Della Valle, E. *Biochim. Biophys. Acta, Proteins Proteomics* **2008**, *1784*, 1454−1461.
(21) Sauer, M.; Haefele, T.; Graff, A.; Nardin, C.; Meier, W. *Chem. Commun. (Cambridge, U. K.)* **2001**, 2452−2453.
(22) Kumar, M.; Grzelakowski, M.; Zilles, J.; Clark, M.; Meier, W. *Proc. Natl. Acad. Sci. U. S. A.* **2007**, *104*, 20719−20724.
(23) Nardin, C.; Thoeni, S.; Widmer, J.; Winterhalter, M.; Meier, W. *Chem. Commun. (Cambridge, U. K.)* **2000**, 1433−1434.
(24) Burke, S. E.; Eisenberg, A. *Polymer* **2001**, *42*, 9111−9120.
(25) de Hoog, H.-P. M.; Vriezema, D. M.; Nallani, M.; Kuiper, S.; Cornelissen, J. J. L. M.; Rowan, A. E.; Nolte, R. J. M. *Soft Matter* **2008**, *4*, 1003−1010.
(26) Kim, K. T.; Winnik, M. A.; Manners, I. *Soft Matter* **2006**, *2*, 957−965.
(27) Roy, D.; Sumerlin, B. S. *ACS Macro Lett.* **2012**, *1*, 529−532.
(28) Gaitzsch, J.; Appelhans, D.; Grafe, D.; Schwille, P.; Voit, B. *Chem. Commun. (Cambridge, U. K.)* **2011**, *47*, 3466−3468.
(29) Gaitzsch, J.; Appelhans, D.; Wang, L.; Battaglia, G.; Voit, B. *Angew. Chem., Int. Ed.* **2012**, *51*, 4448−4451.
(30) Yassin, M. A.; Appelhans, D.; Mendes, R. G.; Rümmeli, M. H.; Voit, B. *Chem.—Eur. J.* **2012**, *18*, 12227−12231.
(31) Meier, W.; Nardin, C.; Winterhalter, M. *Angew. Chem., Int. Ed.* **2000**, *39*, 4599−4602.
(32) Ayfer, B.; Dizman, B.; Elasri, M. O.; Mathias, L. J.; Avci, D. *Des. Monomers Polym.* **2005**, *8*, 437−451.
(33) Zhang, H.; Li, C.; Guo, J.; Zang, L.; Luo, J. *J. Nanomater.* **2012**, *2012*, Article ID 217412.
(34) Prucker, O.; Naumann, C. A.; Rühe, J.; Knoll, W.; Frank, C. W. *J. Am. Chem. Soc.* **1999**, *121*, 8766−8770.
(35) Rich, P. R.; Iwaki, M. *Biochemistry (Moscow)* **2007**, *72*, 1047−1055.
(36) Veitch, N. C. *Phytochemistry* **2004**, *65*, 249−259.
(37) Sigg, S. J.; Seidi, F.; Renggli, K.; Silva, T. B.; Kali, G.; Bruns, N. *Macromol. Rapid Commun.* **2011**, *32*, 1710−1715.
(38) Walde, P.; Guo, Z. *Soft Matter* **2011**, *7*, 316−331.
(39) Hollmann, F.; Arends, I. W. C. E. *Polymers* **2012**, *4*, 759−793.
(40) Battaglia, G.; Ryan, A. J. *J. Phys. Chem. B* **2006**, *110*, 10272−10279.
(41) Stauch, O.; Schubert, R.; Savin, G.; Burchard, W. *Biomacromolecules* **2002**, *3*, 565−578.
(42) Egelhaaf, S. U.; Schurtenberger, P. *J. Phys. Chem.* **1994**, *98*, 8560−8573.
(43) Dietliker, K.; Broillet, S.; Hellrung, B.; Rzadek, P.; Rist, G.; Wirz, J.; Neshchadin, D.; Gescheidt, G. *Helv. Chim. Acta* **2006**, *89*, 2211−2225.
(44) Xu, J. J.; Wang, G.; Zhang, Q.; Xia, X. H.; Chen, H. Y. *Chin. Chem. Lett.* **2005**, *16*, 523−526.
(45) Morawski, B.; Lin, Z.; Cirino, P.; Joo, H.; Bandara, G.; Arnold, F. H. *Protein Eng.* **2000**, *13*, 377−384.
(46) Childs, R. E.; Bardsley, W. G. *Biochem. J.* **1975**, *145*, 93−103.
(47) van der Loos, C. M. *J. Histochem. Cytochem.* **2008**, *56*, 313−328.
(48) Caramori, S. S.; Fernandes, K. F.; de Carvalho Junior, L. B. *Sci. World J.* **2012**, Article ID 129706.
(49) Fanjul-Bolado, P.; Gonzalez-Garcia, M. B.; Costa-Garcia, A. *Anal. Bioanal. Chem.* **2005**, *382*, 297−302.
(50) http://www.chemicalbook.com/ChemicalProductProperty_EN_CB6107909.htm.
(51) Gallati, H. *J. Clin. Chem. Clin. Biochem.* **1979**, *17*, 1−7.
(52) Cattaneo, M. V.; Luong, J. H. T. *Anal. Biochem.* **1994**, *223*, 313−320.
(53) Frej, H.; Daszkiewicz, Z.; Kyziol, J. B. *Chem. Pap.* **1990**, *44*, 191−199.
(54) Goodwin, D. C.; Yamazaki, I.; Aust, S. D.; Grover, T. A. *Anal. Biochem.* **1995**, *231*, 333−338.
(55) Battaglia, G.; Ryan, A. J.; Tomas, S. *Langmuir* **2006**, *22*, 4910−4913.
(56) Berginc, K.; Žakelj, S.; Levstik, L.; Uršič, D.; Kristl, A. *Eur. J. Pharm. Biopharm.* **2007**, *66*, 281−285.
(57) Nardin, C.; Hirt, T.; Leukel, J.; Meier, W. *Langmuir* **2000**, *16*, 1035−1041.
(58) Nehring, R.; Palivan, C. G.; Casse, O.; Tanner, P.; Tüxen, J.; Meier, W. *Langmuir* **2008**, *25*, 1122−1130.